IIETA International Information and Engineering Technology Association
Advancing the World of Information and Engineering

Annales de Chimie - Science des Matériaux
Vol. 46, No. 4, August, 2022, pp. 213-221
Journal homepage: http://iieta.org/journals/acsm

Investigation of Hydrothermal Aging on Polyvinyl Chloride (PVC) Used in Medium Voltage Cables

Hassene Ait Ouazzou[1*], Mohammed Nedjar[1], Smain Hocine[2], Rachid Belhocine[3], Ferhat Belabbas[4]

[1] Laboratoire de Génie Electrique (LGE), Université Mouloud Mammeri de Tizi-Ouzou, Tizi-Ouzou 15000, Algeria
[2] Laboratoire de Chimie Appliquée et Génie Chimique (LCAGC), Université Mouloud Mammeri de Tizi-Ouzou, Tizi-Ouzou 15000, Algeria
[3] Les câbleries électriques d'Alger, Alger 16000, Algeria
[4] Entreprise Electro-industries, Azazga, Tizi-Ouzou 15000, Algeria

Corresponding Author Email: aitouazzou.hassene@outlook.fr

https://doi.org/10.18280/acsm.460407

Received: 21 July 2022
Accepted: 20 August 2022

Keywords:
polyvinyl chloride, hydrothermal aging, electrical properties, mechanical properties, degradation

ABSTRACT

This investigation deals with the effect of hydrothermal aging on the electrical insulating properties of polyvinyl chloride used in medium voltage cables. The evolution of dielectric properties (dielectric loss factor, dielectric constant, dielectric strength and volume resistivity) as a function of aging time and temperature has been studied. After that, the mechanical characteristics (elongation at break and tensile strength) were also determined. Physico-chemical analysis was performed to highlight the structural changes induced by hydrothermal aging. Infrared spectroscopy using the Fourier transform (ATR-FTIR) and thermogravimetric analysis (TGA-DTA) have been performed. The results obtained show that the loss factor and dielectric constant increase gradually with the increase of temperature, while the volume resistivity decreases. At 100°C, the general shape of the curves giving the evolution of dielectric properties as a function of aging time shows that both loss factor and dielectric constant increase while those of volume resistivity and dielectric strength decrease. In the case of 80°C, the loss factor decreases slightly and the dielectric constant remains almost constant with aging time, whereas the volume resistivity and dielectric strength increase. The activation energy varies with aging time. The impact of hydrothermal aging on the properties of the material has been established in this study. At the beginning of aging, the degradation is mainly due to the elimination of molecular HCl. At more advanced stages of aging, the degradation is attributed to the elimination of HCl and double bonds formation followed by a change in color. Other consequences of the degradation like crosslinking and swelling of the samples are also noticed.

1. INTRODUCTION

Polymeric materials are extensively employed in industrial and home life for various purposes. This large range of use of polymers stimulated academic and industry attention, with emphasis on new properties and prospective applications of these materials [1].

Today, polyvinyl chloride (PVC) is still one of the essential plastics worldwide. It is used for a wide range of applications. Among polymers, this material accounts for a high proportion because of its excellent properties. Furthermore, it has the advantage of low cost and high versatility. Cables constitute one of the most significant market applications for polyvinyl chloride (PVC). It is well known that electrical cables are commonly employed in metropolitan areas for electrical transport and distribution networks. Thus, increasing emphasis has been placed on the continual development of novel insulating materials in medium and high voltage cables [2-4]. Nevertheless, irreversible changes might occur due to the degradation after exposing these insulation materials to thermal, moisture, mechanical and electrical stresses during the operating conditions of power cables leading to the progressive deterioration of the characteristics of initial material and thence to the shortening of its lifetime [4-6].

Temperature and humidity are the primary stressors that may adversely impact the performance of these dielectric materials, causing irreversible degradation via thermal aging, hydrolytic aging, or a combination of the two (hydrothermal aging). In assessing electrical insulating materials, these diverse forms of aging are critical.

Gonon et al. [7] proved that combined effects of humidity and thermal stress have a serious impact on the dielectric properties of epoxy-silica composites. It has been shown that water absorption rises with cure, when the dielectric constant is reduced and the loss factor increases. Hui et al. [8] demonstrated that hydrothermal aging causes the reduction of the electrical performance of the XLPE/silica nanocomposites. Roggendorf et al. [9] evaluated the variation of dielectric properties of polyamide as a function of aging times such as dielectric loss factor, dielectric constant and dielectric strength. It was found that higher water absorption in the pressure cooker leads to higher dielectric constant and loss factor and lower dielectric strength.

Literature studies prove that the mechanical properties deteriorate because of micro-crack formation due to uneven thermal contraction and expansion at hydrothermal conditions

[10, 11]. Sebbane et al. [12] have reported that the degradation of mechanical characteristics of XLPE is mainly due to the chain scission caused by the thermo-oxydation of the material. It has been demonstrated that reduction in mechanical characteristics and water penetration rate is more significant than a rise in temperature at which the material has aged. In addition, the infiltration of water leads to a deterioration that is more characterized by plasticization than by chemical deterioration (hydrolysis). Yin et al. [13] have reported that the tensile strength and elongation at break of Vinylester Resin for Fiber-Reinforced Polymer Composites may be decreased for a prolonged duration of immersion. Djedjlli et al. [14] have reported that combined action of water and temperature induces no significant changes in mechanical properties. According to Larbi et al. [15] and Aldajah et al. [16], the hydrothermal aging of polymeric materials can induce a loss of rigidity and a loss of resistance to breaking, but a gain in ductility (larger elongation or strain at break) due to swelling phenomenon. Various investigations of hydrothermal aging of polyesters and polyamides have been conducted [17, 18], but few articles were devoted to PVC.

Oxidation, the effect of water penetration, loss or migration of plasticizers, and dehydrochlorination are among the different aging mechanisms responsible for the decrease of electrical and mechanical properties [19-23].

The dielectric and mechanical properties of the material such as, loss factor, dielectric constant, volume resistivity, dielectric strength, elongation at break and tensile strength, have been investigated after hydrothermal aging. The aging experiments have been monitored under artificial conditions applied to accelerate the aging. ATR-FTIR and TGA-DTG analysis have also been conducted in order to give more insight of the study. The findings show that dielectric and mechanical properties are affected by hydrothermal aging for both aging temperatures 100°C and 80°C. This impact is more significant in the case of 100°C. Furthermore, among the main factors affecting the degradation of PVC are dehydrochlorination and plasticizer migration.

2. MATERIAL AND METHODS

2.1 Material

The polymer resin is produced by the American company INC USA SHEINTECH SE 1200 ITOCHU. It is marketed under the name PVC-S-70. Its density varies between 0.451 g/cm^3 and 0.601 g/cm^3. Additives are added to the resin. The formulation of the mixture is as follows:

- PVC, 100 parts
- Plasticizer: Di-isodecycle phthalate (DIDP), 45 parts
- Filler $CaCO_3$, 10 parts
- Stabilizer calcium zinc Ca/Zn, 5 parts

The PVC resin and the various additives were introduced into a mixer whose cylinders were heated to 140°C until a paste was obtained. The material, in the form of shreds, was cut into square plates of about 20 cm and 2 mm thickness. These were placed between the plates of a press, heated to 160°C, for 5 min, with press force of 400 kN. Circular specimens with a diameter of 7.5 cm were made for the electrical tests. For the mechanical testing, 7.5 cm long dumbbell-shaped specimens were cut according to the IEC 540 publication's specifications [24].

2.2 Hydrothermal aging

Hydrothermal aging was performed by immersing the different samples in a container containing water. The whole set was introduced into ventilated air ovens with temperatures set at 80°C and 100°C. The water was renewed every 24 h. The aging time reached 15000 h and 10000 h for the temperatures 80°C and 100°C respectively. Samples were taken every 500 hours. The test samples were put in a desiccator before the trials to ensure that there was no moisture present.

2.3 Measurements of electrical properties

To measure the dielectric loss factor and the dielectric constant of the insulation, we used a Schering bridge type TETTEX 2830/2831. The bridge consists of two heating plates that can raise the temperature up to 250°C. The system is equipped with a temperature controller. The measuring device is connected to a computer. The sample was placed between two circular stainless steel electrodes with a surface area of 20 cm^2. A set of weights exerted a pressure of 750 g/cm^2 on the assembly to avoid the presence of air between the specimen and the electrodes. These tests were performed under an AC voltage of 2 kV, 50 Hz. The insulation resistance of the polymer was measured using a pico-amperemeter integrated into the Schering bridge. The measurement was performed at 2 kV DC voltage. The sample temperature varies from 20°C to 140°C with steps of 10°C using a potentiometric temperature regulator monitored by computer. Three samples were tested for dielectric loss factor, dielectric constant, and volume resistivity at each aging period. For each parameter, an average of three values was determined. The breakdown tests were carried out at room temperature using a high voltage AC generator, type BAUR OLPRUFGERAT PGO, 90 A, which can supply a voltage of up to 90 kV at 50 Hz. The electrodes used are made of brass, flat and of Rogowski type. The test cell containing the electrode arrangement is filled with insulating oil (Borak 22) to prevent bypassing. The rate of rise of the voltage ramp is 2 kV/s, and the oil is stirred during all the tests.

2.4 Measurements of mechanical properties

The specimen was traction-broken using an MTS Criterion type 42 traction apparatus for the testing. The dynamometer has two jaws and moves at a speed of 200 mm/min to apply increasing force. The value of extensometer gage length is 20 mm. The dumbbell's dimensions (width and thickness in millimeters) are also inserted into the machine's software. A computer is used as the measurement apparatus. The tests were carried out at room temperature without the need of special equipment. Tensile strength and elongation at break were measured. The tensile strength was calculated as force at the break per unit cross-sectional area of the sample in N/mm^2. The elongation at break, also called strain at break, is the ratio of the modified length to the initial length after the breakage of the specimen. The following relationship gives the property of elongation at break expressed in %:

$$\Delta L\ (\%) = \frac{L - L_0}{L_0} \qquad (1)$$

where:

- L_0: Length separating the two marks delimiting the

calibrated zone before breaking (L_0 = 20 mm).
- L: Length separating the two markers delimiting the calibrated area after breakage [mm].
- ΔL : Elongation at break [%].

The tensile test was performed on six specimens at various aging time. Average values of tensile strength and elongation at break respectively were determined.

2.5 Spectroscopy ATR-FTIR

The adaptable ATR-FTIR approach may be used to emphasize the chemical alterations brought on by hydrothermal aging. A ATR-FTIR Agilent Cary 630 type spectrometer was used in our work to evaluate materials with a thickness of 2 mm. Unaged and aged specimens were scanned with a resolution of 4 cm^{-1} in the spectral region of 650-4000 cm^{-1}. Seventy four scans were performed for each specimen.

2.6 Thermogravimetry analysis (TGA-DTA)

The decomposing process was monitored with a TA Instruments SDT Q600 thermal analyzer. A quantity of 7.771 mg of the material was put in an alumina crucible for each test. All of the tests were carried out in a nitrogen environment with a 50 mL/min flow rate. The samples were heated at a steady rate of 10°C/min between 30°C and 900°C for the analysis.

3. RESULTS AND DISCUSSION

3.1 Variation of electrical characteristics as a function of aging time

3.1.1 Dielectric loss factor

Figure 1 shows the variation of the dielectric loss factor as a function of aging time. At 100°C, the characteristic is irregular with the presence of four peaks corresponding to an aging time of 1000 h, 3500 h, 5000 h and 6500 h, slowly decreasing after 8000 h of aging. On the 80°C curves, there are four peaks corresponding to aging times of 1000 h, 3500 h, 6500 h and 10000 h. After 10000 h, the dielectric loss factor decreases slightly until an aging time of 15000 h.

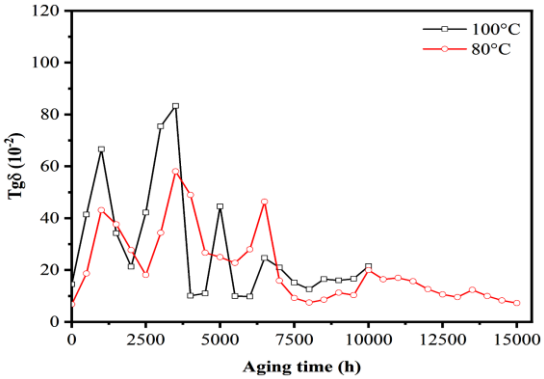

Figure 1. Variation of the dielectric loss factor versus the aging time

3.1.2 Dielectric constant

The evolution of the dielectic constant (ε_r) as a function of aging time is shown in Figure 2. At 100°C, ε_r increases from 7.36 to 9.66 after 1000 h of aging. It then slightly decreases and reaches a value of 8.45 after 2000 h. The curve of ε_r shows a non-monotonic variation from 2000 h to reach a value of 10.754 after 7000 h of aging. Beyond this time the dielectic constant increases sharply and reaches a value of 25.52 corresponding to 10000 h of aging. At 80°C, ε_r decreases to 7.06. It then increases slightly from 500 h and reaches two peaks of 8.72 and 9.64 after an aging time of 3500 h and 8000 h, respectively. Beyond this time, ε_r decreases slightly and remains almost constant.

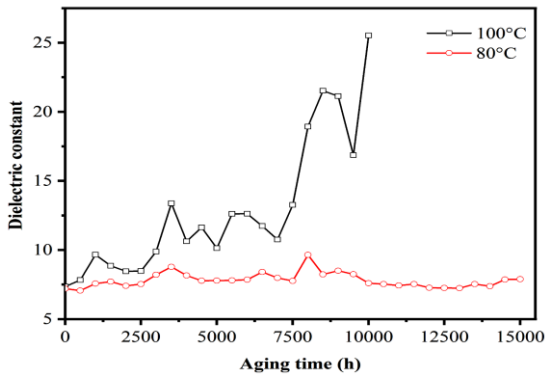

Figure 2. Variation of the dielectric constant versus the aging time

3.1.3 Volume resistivity

Figure 3 represents the variation of volume resistivity with aging time. At 100°C, the volume resistivity was 7.995 x 10^{10} (Ω.cm) before aging. This property decreases considerably after 3000 h to reach a minimum value of 6.51 x 10^9 (Ω.cm). Beyond this time, the curve presents a non-monotonic variation with fluctuations to reach 6.70 x 10^{10} (Ω.cm) corresponding to 10000 h of aging. At 80°C, resistivity decreases rapidly from 3.01 x 10^{11} (Ω.cm) and reaches a minimum value of 2.50 x 10^{10} (Ω.cm) after 1000 h of aging. In the interval of 1000 h and 6500 h, the curve shows a non-monotonic variation with fluctuations to reach a value of 4.513 x 10^{10} (Ω.cm). We note that from 7000 h, it increases considerably to reach a value of 7.11 x 10^{11} (Ω.cm) corresponding to 8000 h of aging. The volume resistivity starts to fluctuate to reach a value of 7.48 x 10^{11} (Ω.cm) after 15000 h of aging.

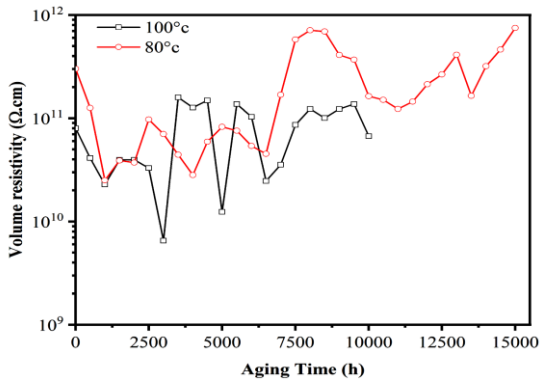

Figure 3. Variation of the volume resistivity versus the aging time

3.1.4 Dielectric strength

Figure 4 represents the variation of the dielectric strength as

a function of aging time. At 100°C, the dielectric strength increases considerably from 16.68 kV/mm to 20.21 kV/mm after 2000 h of aging and then the dielectric strength decreases to 17.42 kV/mm. The dielectric strength increases and reaches a maximum value corresponding to 21.7 kV/mm after 3500 h of aging and then decreases considerably to reach a value of 48.81 kV/mm at 7000 h. Then the dielectric strength increases again and reaches a value of 20.46 kV/mm. Beyond this time, it decreases rapidly and reaches a minimum value of 13.94 kV/mm after 10,000 hours of aging. At 80°C, the dielectric strength increases from 16.68 kV/mm to 17.75 kV/mm for an aging time of 500 h. Beyond this time, the curve presents non-monotonic variations with fluctuations to reach a 20.16 kV/mm value after 15000 h of aging.

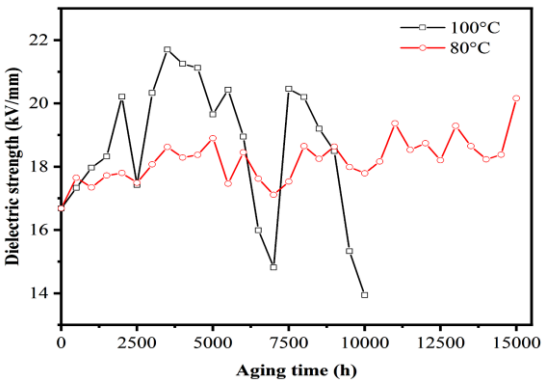

Figure 4. Variation of the dielectric strength versus the aging time

3.2 Variation of mechanical properties as a function of aging time

3.2.1 Elongation at break

Figure 5, shows the variation of the elongation at break as a function of aging time. At 100°C, the value of the elongation at break was 233% before aging. It then decreases considerably and reaches a minimum value of 80.13% after 8500 h of aging. Beyond this time the elongation increases slightly to reach a value of 93.35% after 10000 h of aging. At 80°C, the elongation increases from 233% to 277% after 500 h of aging and beyond this time the curve presents a non monotonous variation with a lot of fluctuation to reach a value of 224.84% at 9000 h. Then the elongation decreases considerably to reach a minimum value of 163.69% at 11000 h. From this time onward, the elongation improves slightly and reaches a value of 211.84% after 15000 h of aging.

3.2.2 Tensile strength

Figure 6 shows the variation of the tensile strength as a function of aging time. At 100°C, tensile strength before aging was 21.83 N/mm^2, and then it started to increase rapidly to reach a maximum value of 24.55 N/mm^2. Beyond this time, the tensile strength decreases considerably until reaching a minimum value corresponding to 19.87 N/mm^2 after 10000 h of aging. At 80°C, before aging, the tensile strength was 21.83 N/mm^2. This value decreases considerably and reaches a minimum value equal to 19.71 N/mm^2 after 500 h of aging. After that, it increases considerably to reach a maximum value of 22.29 N/mm^2 after 5000 h of aging. Beyond this time, the curve presents a non-monotonic variation with a lot of fluctuation to reach a 21.74 N/mm^2 after 15000 h of aging.

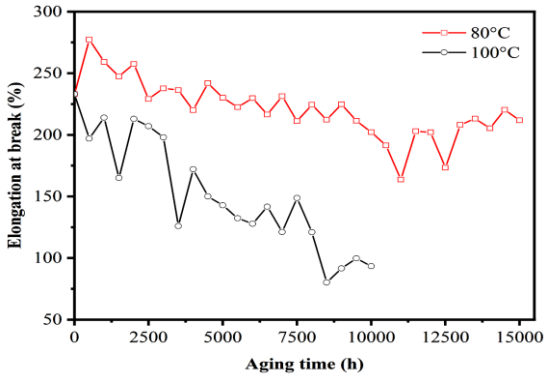

Figure 5. Variation elongation at break as a function of aging time

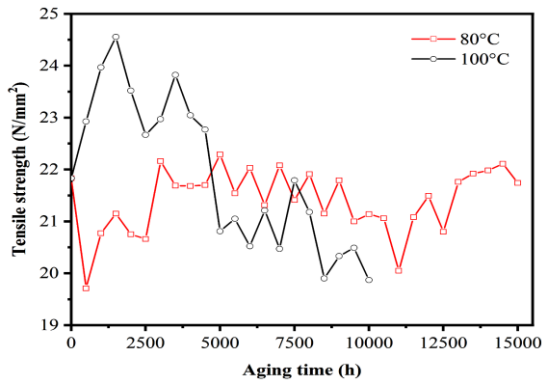

Figure 6. Variation of tensile strength versus aging time at 100°C and 80°C

3.3 Variation in electrical characteristics as a function of Temperature

3.3.1 Dielectric loss factor

Figure 7 shows the evolution of the dielectric loss factor as a function of temperature before and after aging. The temperature varied from 20°C to 140°C. Before aging, Tgδ decreases from 8.96 x 10^{-2} to 5.77 x 10^{-2} at a temperature of 70°C, and then it slowly increases and reaches a value of 53.27 x 10^{-2} at 140°C. At 100°C, the Tgδ increases gradually from 6.2 x 10^{-2} to 35.25 x 10^{-2} at a temperature of 80°C. Beyond this temperature, the Tgδ increases rapidly to 323.67 x 10^{-2} at 140°C. At 80°C, Tgδ increases slightly from 4.54 x 10^{-2} to 7.89 x 10^{-2} and then decreases slowly to 7.24 x 10 $^{-2}$ for a temperature of 80°C. Beyond this temperature, Tgδ increases rapidly and reaches a value of 219.67 x 10^{-2} at a temperature of 140°C.

3.3.2 Dielectric constant

Figure 8 shows the variation of dielectric constant with temperature before and after aging. The temperature varied from 20°C to 140°C. Before aging, the dielectric constant ε_r increases slowly from 4.501 to 7.604 for a temperature of 140°C. At 100°C, the dielectric constant ε_r increases rapidly from 9.012 to 26.199 at a temperature of 110°C. It then decreases to 21.78, corresponds to the temperature of 130°C and then increases again and reaches a value of 23.22 at a temperature of 140°C. After aging for 15000 h at 80°C, the dielectric constant increases rapidly from 3.72 to 10.84, at a temperature of 140°C.

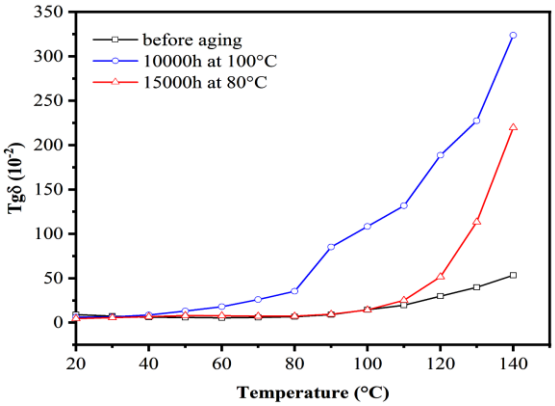

Figure 7. Variation of dielectric loss factor versus temperature before aging, at 100°C and at 80°C

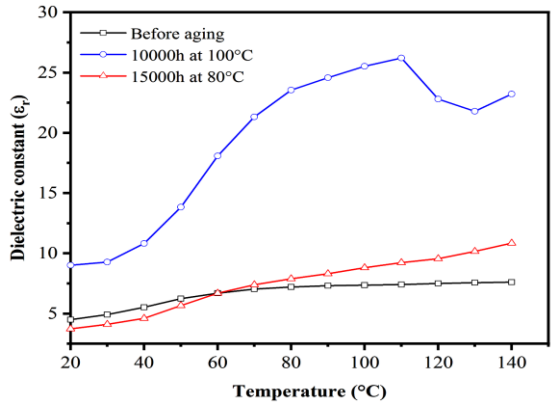

Figure 8. Variation of the dielectric constant versus temperature before aging, at 100°C and at 80°C

3.3.3 Volume resistivity

Figure 9 shows the variation of volume resistivity with temperature before and after aging. The range of temperature variation is from 20°C to 140°C. Before aging, the volume resistivity increases from 8.22 x 10^{12} (Ω.cm) to 4.45 x 10^{13} (Ω.cm) and then decreases to 7.995 x 10^{10} (Ω.cm) at a temperature of 100°C. Then the volume resistivity increases slightly to 1.029 x 10^{11} (Ω.cm) at a temperature of 110°C. Beyond this temperature, the resistivity decreases to a value of 3.94 x 10^{10} (Ω.cm), at the temperature of 140°C. At 80°C, the resistivity remains almost constant until 40°C. It then decreases rapidly and reaches a value of 1 x 10^{10} (Ω.cm) at 140°C.

To properly analyze the resistivity behaviour, we plotted the volume resistivity as a function of the inverse of the absolute temperature before and after aging times of 15000 h and 10000 h at 80 and 100°C, respectively (Figure 10). The results show that the volume resistivity decreases linearly with temperature. These straight lines obey Arrhenius' law, which is true for the volume resistivity ρ.

$$\rho = \rho_{\infty} \exp\left(^{-E_a}/_{RT}\right) \qquad (2)$$

where:

- ρ_{∞} (Ω.cm) is the limit of the value of the resistivity at infinite temperature.
- E_a (J.mol^{-1}) is the activation energy of the process.
- T (K) is the absolute temperature.
- R is the gas constant (R = 8,314 J.mol^{-1}.K^{-1}).

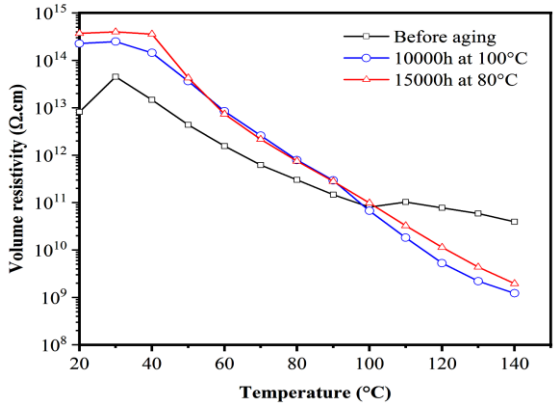

Figure 9. Variation of the volume resistivity versus the temperature before aging, at 100°C and at 80°C

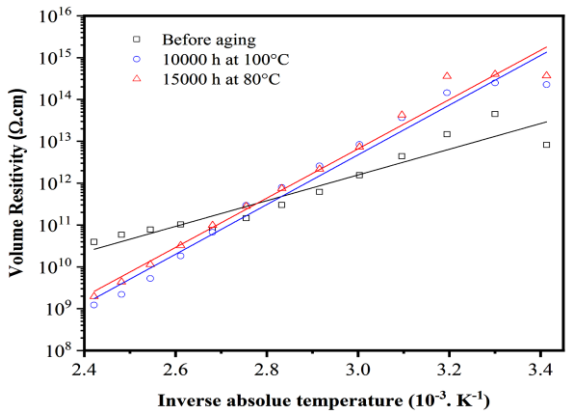

Figure 10. Variation of volume resistivity versus inverse of absolute temperature (x10^{-3} K^{-1}) at 80°C and at 100°C

The values of the activation energy before and after aging are shown in Table 1.

Table 1. Values of the activation energy (kcal/mol)

Aging Time (h)	Activation Energy (kcal/mol)
Before aging	25.54
10000 at 100°C	49.38
15000 at 80°C	48.96

4. ATR-FTIR SPECTROSCOPY RESULTS

The ATR-FTIR absorbance spectra of unaged (virgin) PVC (black) and aged PVCs for 15000 hours (red) and 10000 hours (blue) recorded between the wavenumbers 4000 cm^{-1} and 600 cm^{-1} are shown in Figure 11. Complete spectra adequately show the characteristic bands of PVC. These bands are from the data found in the literature for PVC.

The absorption bands observed in ATR-FTIR spectra before and after aging at 80 and 100°C are given in Figure 11. In the spectrum of the untreated sample, the main peaks at 2850 - 2950 cm^{-1}, 1255-1275 cm-^{1}, 1425-1458 cm^{-1} and 741 cm^{-1}, characteristic for a PVC structure, were found, which are attributed to C-H (valence), C-C (valence), C-H (deformation), and C-Cl valance bands, respectively [25-32]. In the FTIR spectra of PVC after treatment at 80°C and 100°C, the intensity of the bands decreased as compared to the untreated sample. Hydrothermal aging reduced the peak intensity of the bands for the stretching of the C-Cl band at 741.9 cm^{-1} and C-H at

2850 - 2950 cm^{-1}. This observation suggests that the PVC structure is altered after hydrothermal aging.

The bands observed around 1720 cm^{-1} and 873 cm^{-1} are attributed to the vibration of C=O groups in plasticizers and $CaCO_3$ (multifunctional additive) respectively [27, 33]. The peak at 3600-3200 cm^{-1} is attributed to the -OH stretching of water (H_2O) [34].

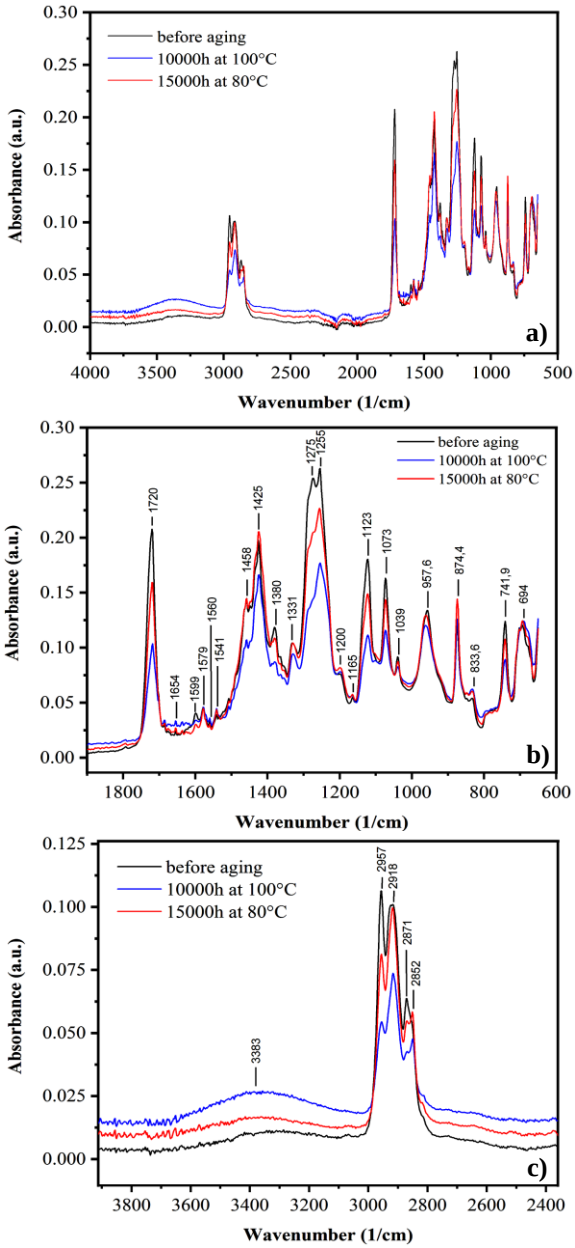

Figure 11. Thermal aging of PVC ATR-FTIR spectra: (a) full spectra; (b) focusing on the absorption bands between 600 and 1900 cm^{-1}; (c) focusing on the absorption bands between 2359 and 3912 cm^{-1}

5. TGA-DTA ANALYSIS RESULTS

Thermogravimetric (TGA-DTA) analysis of the unaged (virgin) PVC (black) and aged PVCs for 15000 hours (red) and 10000 hours (blue) shows two mass loss (Figure 12). The first signal between 100°C and 300°C corresponding to the departure of HCl (dechlorination) accounts for about 60% of the total weight loss. A second mass loss at temperatures between 300°C and 450°C, is attributed to hydrocarbons as a polyene-like structure with the total weight loss of 15%.

This step involves pyrolysis of the polyene structure, yielding mainly to the formation of coke.

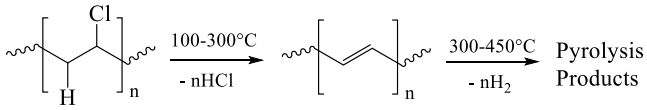

In differential thermal (DT) analysis, the loss of HCl and polyene structure corresponds to endothermic peaks at 290°C and 450°C.

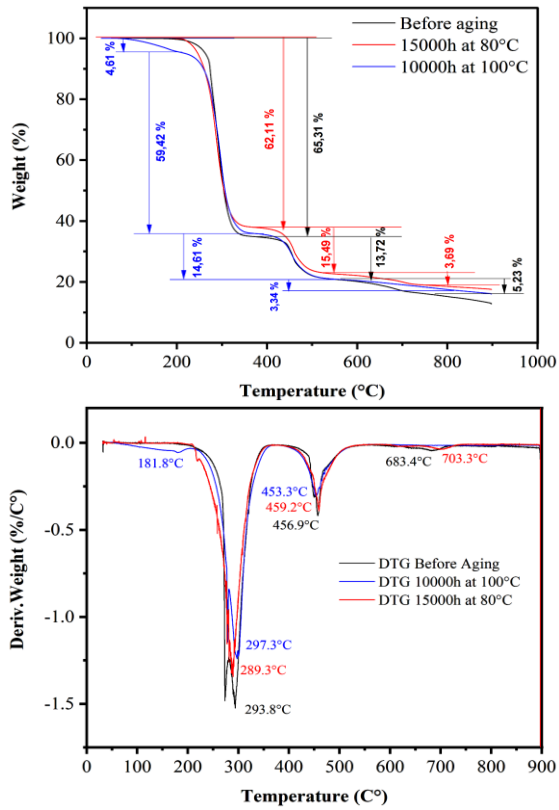

Figure 12. TGA and DTA curve for: Before aging, 15000 h at 80°C and 10000 h at 100°C

6. CHANGES IN COLOR

The degradation occurs with elimination of HCl and is accompanied by a change in color. The samples are colored due to the removal of an HCl molecule which leads to the formation of conjugated double bonds in the PVC [35]. As soon as the conjugation index is around 4-5, the structure absorbs part of the spectrum of visible light: the material is colored. As the loss of HCl intensifies over time, the conjugation index also increases. It quickly changes from a pale yellow color for the unaged sample (a) to dark brown color for the aged sample at 100°C (c) as shown in Figure 13.

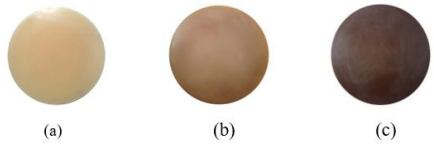

Figure 13. Color change of PVC samples: a) unaged, b) aged for 15000 h at 80°C, c) aged for 10000 h at 100°C

7. DISCUSSIONS

The results obtained show the variation of electrical and mechanical properties of PVC versus the aging time and temperature, respectively. These properties are: dielectric loss factor, dielectric constant, volume resistivity, dielectric strength, elongation at break, tensile strength, ATR-FTIR and TGA-DTA.

- The variation of dielectric loss factor and dielectric constant has similar behavior with aging time. Their increase is attributed to the double bonds formation after removal of HCl, leading to alternating single and double bonds [36, 37]. This structure is what makes them conductive as they allow electrical charge to move along their monomer chain leading to a considerable augmentation in the conductivity, whereas, their decrease is due to rearrangements of the polymer's molecular chains, expressing a reduction in the polymer conductivity. At 80°C the dielectric constant remains stable during all the aging time, which explains that double bonds responsible for the loss of the dielectric constant are not formed at this temperature as confirmed by the results of thermogravimetry (Figure 12).
- The augmentation of the volume resistivity is probably due to the reduction of the mobility of charge carriers, while the diminution is attributed to a dehydrochlorination phenomenon, which leads to the formation of double bonds and release of HCl molecules from the PVC polymer chains under temperature effect [38]. The decrease of volume resistivity is more pronounced in the case of 100°C because of the number of charge carriers created by the loss of HCl, which is higher compared to 80°C. This loss of HCl is confirmed by the ATR-FTIR and TGA analyses.
- The rigidity of the material depends on the number of unsaturation (double bonds) formed during aging. In the case of 100°C, the number of double bonds is more important compared to the one treated at 80°C. This behavior explains the significant decrease in the dielectric strength of the polymer at 100°C.
- The drop in mechanical properties (elongation at break and tensile strength) is attributed to the increase in the number of unsaturation of the material. This decrease is more accentuated in the case of 100°C. The reduction of mechanical properties can also be explained by the loss of plasticizer which is confirmed by the ATR-FTIR.
- From Figure 10, the activation energy (E_a) can be estimated. The value is 25.54 kcal/mol before aging. It grows to 48.96 kcal/mol and 49.38 kcal/mol for 15000 hours at 80°C and 10000 hours at 100°C, respectively. As a result, the activation energy varies with aging. This phenomenon is likely attributable to the variation in chemical reaction rates of HCl elimination, which become more pronounced after aging. These results are consistent with those published elsewhere. Morel et al. [39] investigated activation energy as functions aging time in polyethylene-terephthalate films.
- The thermal stability of PVC decreases with aging time due to the loss of HCl. According to the results shown in Figure 12, the material aged at 100°C is the least stable compared to the material aged at 80°C and/or the unaged material.

Among the main processes that cause the degradation of PVC are dehydrochlorination and loss of plasticizer.

PVC degradation occurs when the material undergoes elevated temperatures that can cause the loss of physical properties, such as optical and mechanical properties. The degradation onset temperature of the unaged and aged PVC at 80°C was around 260°C but for the sample aged at 100°C, degradation begins before 200°C (Figure 12). Chlorine content in polyvinyl chloride is approximately 56.7%, it is released as HCl gas when PVC is heated at 300°C. Thermogravimetric data showed that the unaged PVC, aged at 80°C and aged at 100°C lost 65.31%, 62.11% and 59.42% of their original mass respectively at 300°C, suggesting that the totality of HCl is removed in the first stage. The TG curve for PVC showed all compounds losing 60% of its weight by 300°C and then a total of 80% by 400°C, suggesting that the evolution of plasticizer occurs in two stages and the polymer undergoes negligible further weight loss in its conversion to coke. This degradation is confirmed by IR analysis. The IR spectrum of PVC showed that the C-H bands (2957 cm^{-1}) of the compound aged at 100°C lost half of their intensity (Figure 11-c). The dechlorination of PVC was evidenced by the decreasing intensity of the C–Cl (750 cm^{-1}) stretching vibration. In addition, the bands at about 1654 cm^{-1} assigned to C=C appeared and the intensity of this band was increased (Figure 11-b) for the aged PVC at 100°C, indicating the elimination of HCl during the hydrothermal dechlorination of PVC. The evolution of HCl results in unsaturation in the polymer chain. The dehydrochlorination appears to progress in stepwise fashion along the polymer chain to produce conjugated unsaturation (b). This leads to color formation in the residue of the aged PVC at 80°C and 100°C (Figure 13.).

The hydrothermal degradation of PVC occurs by a radical mechanism and exhibits two reaction types of degradation (Figure 14): elimination (path 1) and substitution (path 2). During the radical mechanism elimination reaction (path 1), between 200 and 360°C, mainly HCl and polyene are formed. The hydroxylation of PVC is obtained by the radical substitution reaction (path 2). During this reaction the Cl atoms are replaced by O-H groups, leading to the formation of alcohol or polyol (c) [34].

The peak at around 3381 cm^{-1} observed in Figure 11(c) assigned to the –OH group confirmed the replacement of –Cl with the –OH group.

The presence of this group (O-H) in the aged samples at 80°C and 100°C, suggests the formation of a hydroxyl group (c) by radical substitution reaction as shown below:

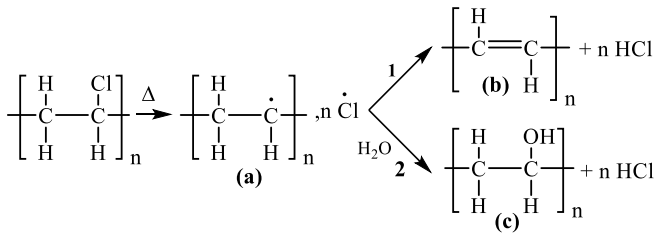

Figure 14. Reaction pathways of PVC degradation

The degradation also affected the plasticizer, the vibration band of the C=O group of the ester function at 1720 cm^{-1} is reduced by half for the compound aged at 100°C. During this process, plasticizer (Di-isodecycle phthalate) decomposes into benzene, alkene and CO_2. As shown in Figure 11(b), the band at 1123 cm^{-1} ascribed to the C-O decreased, indicating the

degradation of the functional group and also the skeletal chain of plasticizer (DIDP). A swelling of PVC has been noticed. This behavior is due to the OH groups formed during the substitution of the chlorine atoms as shown by the products (c) of the chemical reaction (path 2- Figure 14).

8. CONCLUSION

In this paper, the effects of hydrothermal aging conditions on PVC's electrical and mechanical properties have been investigated. This work shows that both properties have been seriously affected by the combined action of temperature and water. Among factors which cause the increase of the dielectric properties (loss factor and dielectric constant) is the formation of double bonds after removal of HCl. On the another hand, the considerable augmentation of the polymer's conductivity is explained by the alternance in single and double bonds caused by removal of HCl, whereas reduction of the loss factor and dielectric constant is due to the rearrangements of the polymer's molecular chains. Because there are more charge carriers produced by the loss of HCl at 100°C than at 80°C, the volume resistivity decreases more noticeably at this temperature. The ATR-FTIR and TGA analyses support this loss of HCl. The material's stiffness is determined by the quantity of unsaturation (double bonds) produced during degradation. Compared to the sample treated at 80°C, the quantity of double bonds in the 100°C conditions is more significant. This phenomenon explains why the polymer's dielectric strength decreases significantly at 100°C. The increase in the number of unsaturations in the material leads to the material's stiffness, which causes a decrease in mechanical properties (elongation at break and tensile strength). In the case of 100°C, this decrease is more pronounced. The loss of plasticizer can be also added to the factors inducing the decrease of mechanical characteristics. The higher activation energy at 100°C can be explained by the higher number of double bonds formed during the aging process. The results obtained show that the material aged at 100°C is the least stable due to the loss of HCl from PVC. The degradation was characterized by outgassing, color change, and swelling of the PVC.

ACKNOWLEDGMENT

We thank Mr EDGARD CHEMALI, Director of Operations of 'Les Câbleries Electriques d'Alger (CABEL)', Gué de Constantine, Algeria for helped make this study possible.

REFERENCES

[1] Suraci, S.V., Fabiani, D., Bulzaga, S., Mazzocchetti, L. (2018). Investigation of thermal degradation of LDPE-based materials through electrical measurements. In 2018 IEEE 2nd International Conference on Dielectrics (ICD), pp. 1-4. https://doi.org/10.1109/ICD.2018.8514643

[2] Kocsis, D., Deák, G., Keki, S., Dezső, G., Horvath, R. (2018). Artificial aging examination of PVC fibers as vibrating strings. Environmental Engineering & Management Journal (EEMJ), 17(11). https://doi.org/10.30638/eemj.2018.255

[3] Wang, Z., Xie, T., Ning, X., Liu, Y., Wang, J. (2019). Thermal degradation kinetics study of polyvinyl chloride (PVC) sheath for new and aged cables. Waste Management, 99: 146-153. https://doi.org/10.1016/j.wasman.2019.08.042

[4] Kemari, Y., Mekhaldi, A., Teguar, M. (2017). Experimental investigation and signal processing techniques for degradation assessment of XLPE and PVC/B materials under thermal aging. IEEE Transactions on Dielectrics and Electrical Insulation, 24(4): 2559-2569. https://doi.org/10.1109/TDEI.2017.006399

[5] Nedjar, M., Béroual, A., Boubakeur, A. (2006). Influence of thermal aging on the electrical properties of poly (vinyl chloride). Journal of Applied Polymer Science, 102(5): 4728-4733. https://doi.org/10.1002/app.24874

[6] Azimuddin, A., Refaat, S.S. (2021). A comprehensive model for electrical degradation of power cable insulation. In 2021 IEEE Conference on Electrical Insulation and Dielectric Phenomena (CEIDP), pp. 133-138. https://doi.org/10.1109/CEIDP50766.2021.9705370

[7] Gonon, P., Sylvestre, A., Teysseyre, J., Prior, C. (2001). Combined effects of humidity and thermal stress on the dielectric properties of epoxy-silica composites. Materials Science and Engineering: B, 83(1-3): 158-164. https://doi.org/10.1016/S0921-5107(01)00521-9

[8] Hui, L., Nelson, J.K., Schadler, L.S. (2010). Hydrothermal aging of XLPE/silica nanocomposites. In 2010 Annual Report Conference on Electrical Insulation and Dielectic Phenomena, pp. 1-4. https://doi.org/10.1109/CEIDP.2010.5724045

[9] Roggendorf, C., Kessler, M., Schulte, S., Schnettler, A. (2010). Accelerated test procedures for hydrothermal aging. In 2010 IEEE International Symposium on Electrical Insulation, pp. 1-5. https://doi.org/10.1109/ELINSL.2010.5549754

[10] Srivastava, V.K. (1999). Influence of water immersion on mechanical properties of quasi-isotropic glass fibre reinforced epoxy vinylester resin composites. Materials Science and Engineering: A, 263(1): 56-63. https://doi.org/10.1016/S0921-5093(98)01037-5

[11] Valarmathi, T.N., Sangeetha, M., Venkata, G.G., Muppala, D., Siva, R. (2021). Hygro-thermal degradation studies on E-glass woven rovings and aramid fiber composites. Materials Today: Proceedings, 44: 3823-3828. https://doi.org/10.1016/j.matpr.2020.12.336

[12] Sebbane, Y., Boubakeur, A., Mekhaledi, A. (2021). Influence of thermal aging and water adsorption on XLPE cables insulation mechanical and physico-chemical properties. IEEE Transactions on Dielectrics and Electrical Insulation, 28(5): 1694-1702. https://doi.org/10.1109/TDEI.2021.009459

[13] Yin, X., Liu, Y., Miao, Y., Xian, G. (2019). Water absorption, hydrothermal expansion, and thermomechanical properties of a vinylester resin for fiber-reinforced polymer composites subjected to water or alkaline solution immersion. Polymers, 11(3): 505. https://doi.org/10.3390/polym11030505

[14] Djidjelli, H., Kaci, M., Boukerrou, A., Benachour, D., Martinez-Vega, J.J. (2003). Hydrothermic aging of plasticized poly (vinyl chloride): Its effect on the dielectric, thermal, and mechanical properties. Journal of

Applied Polymer Science, 89(13): 3447-3457. https://doi.org/10.1002/app.12554
[15] Larbi, S., Bensaada, R., Djebali, S., Bilek, A. (2016). Experimental and theoretical study on hygrothermal aging effect on mechanical behavior of fiber reinforced plastic laminates. International Journal of Mechanical, Aerospace, Industrial, Mechatronic and Manufacturing Engineering, 10(7): 1239-1242. https://doi.org/10.5281/zenodo.1125411
[16] Aldajah, S., Alawsi, G., Rahmaan, S.A. (2009). Impact of sea and tap water exposure on the durability of GFRP laminates. Materials & Design, 30(5): 1835-1840. https://doi.org/10.1016/j.matdes.2008.07.044
[17] Abeysinghe, H.P., Edwards, W., Pritchard, G., Swampillai, G.J. (1982). Degradation of crosslinked resins in water and electrolyte solutions. Polymer, 23(12): 1785-1790. https://doi.org/10.1016/0032-3861(82)90123-9
[18] Pritchard, G., Speake, S.D. (1987). The use of water absorption kinetic data to predict laminate property changes. Composites, 18(3): 227-232. https://doi.org/10.1016/0010-4361(87)90412-5
[19] Nedjar, M., Boubakeur, A., Beroual, A., Bournane, M. (2003). Thermal aging of polyvinyl chloride used in electrical insulation. Annales de Chimie Science des Matériaux, 28(5): 97-104. https://doi.org/10.1016/S0151-9107(03)00109-0
[20] Ekelund, M., Edin, H., Gedde, U.W. (2007). Long-term performance of poly (vinyl chloride) cables. Part 1: Mechanical and electrical performances. Polymer Degradation and Stability, 92(4): 617-629. https://doi.org/10.1016/j.polymdegradstab.2007.01.005
[21] Plaček, V., Kohout, T. (2010). Comparison of cable ageing. Radiation Physics and Chemistry, 79(3): 371-374. https://doi.org/10.1016/j.radphyschem.2009.08.031
[22] Royaux, A., Fabre-Francke, I., Balcar, N., Barabant, G., Bollard, C., Lavédrine, B., Cantin, S. (2017). Aging of plasticized polyvinyl chloride in heritage collections: The impact of conditioning and cleaning treatments. Polymer Degradation and Stability, 137: 109-121. https://doi.org/10.1016/j.polymdegradstab.2017.01.011
[23] Kemari, Y., Mekhaldi, A., Teguar, M., Teyssedre, G. (2019). AC conductivity analysis and chemical changes of thermally aged PVC/B insulation for medium voltage cables. In 11th National Conference on High Voltage (CNHT), Oran, Algeria, pp. 1-4. https://hal.archives-ouvertes.fr/hal-02397501.
[24] IEC 540. (1976). Tests for Insulations and Sheaths of Electric Cables and Cords (Elastomeric and Thermoplastic Compounds).
[25] Amar, Z.H., Chabira, S.F., Sebaa, M., Ahmed, B. (2019). Structural changes undergone during thermal aging and/or processing of unstabilized, dry-blend and rigid PVC, investigated by FTIR-ATR and curve fitting. In Annales de Chimie: Science des Materiaux, 43(1): 59-68. https://doi.org/10.18280/acsm.430109
[26] Gaballah, S.T., Khalil, A.M., Rabie, S.T. (2019). Thiazole derivatives-functionalized polyvinyl chloride nanocomposites with photostability and antimicrobial properties. Journal of Vinyl and Additive Technology, 25(S1): E137-E146. https://doi.org/10.1002/vnl.21670
[27] Ivanov, V.B., Solina, E.V., Staroverova, O.V., Popova, E.I., Lazareva, O.L., Belova, O.A. (2017). Influence of external conditions on the relation between the physical and chemical processes in the thermodegradation of plasticized poly (vinyl chloride). Russian Journal of Physical Chemistry B, 11(6): 978-984. https://doi.org/10.1134/S1990793117060033
[28] Machado, M.C., Webster, T.J. (2017). Lipase degradation of plasticized polyvinyl chloride endotracheal tube surfaces to create nanoscale features. International Journal of Nanomedicine, 12: 2109. https://doi.org/10.2147/IJN.S130608
[29] Tabb, D.L., Koenig, J.L. (1975). Fourier transform infrared study of plasticized and unplasticized poly (vinyl chloride). Macromolecules, 8(6): 929-934. https://doi.org/10.1021/ma60048a043
[30] Djouani, F., Mkacher, I., Colin, X., Brument, Y., Cristiano-Tassi, A. (2014). Evaporation kinetics of DIDP plasticizer from PVC. In AIP Conference Proceedings, 1599(1): 218-221. https://doi.org/10.1063/1.4876817
[31] Lobo, H., Bonilla, J.V. (Eds.). (2003). Handbook of Plastics Analysis, 68. https://doi.org/10.1201/9780203911983
[32] Chen, J., Nie, X.A., Jiang, J.C., Zhou, Y.H. (2018). Thermal degradation and plasticizing mechanism of poly (vinyl chloride) plasticized with a novel cardanol derived plasticizer. In IOP Conference Series: Materials Science and Engineering, 292(1): 012008. https://doi.org/10.1088/1757-899X/292/1/012008
[33] Salivon, T., Colin, X., Comte, R. (2015). Degradation of XLPE and PVC cable insulators. In 2015 IEEE Conference on Electrical Insulation and Dielectric Phenomena (CEIDP), pp. 656-659. https://doi.org/10.1109/CEIDP.2015.7352022
[34] Lu, J., Ma, S., Gao, J. (2002). Study on the pressurized hydrolysis dechlorination of PVC. Energy & Fuels, 16(5): 1251-1255. https://doi.org/10.1021/ef020048t
[35] Bouchoul, B., Benaniba, M.T., Massardier, V. (2014). Effect of biobased plasticizers on thermal, mechanical, and permanence properties of poly (vinyl chloride). Journal of Vinyl and Additive Technology, 20(4): 260-267. https://doi.org/10.1002/vnl.21356
[36] Chiang, C.K., Fincher Jr, C.R., Park, Y.W., Heeger, A.J., Shirakawa, H., Louis, E.J., MacDiarmid, A.G. (1977). Electrical conductivity in doped polyacetylene. Physical Review Letters, 39(17): 1098. https://doi.org/10.1103/physrevlett.39.1098
[37] Naarmann, H., Theophilou, N. (1987). New process for the production of metal-like, stable polyacetylene. Synthetic Metals, 22(1): 1-8. https://doi.org/10.1016/0379-6779(87)90564-9
[38] Quennehen, P., Royaud, I., Seytre, G., Gain, O., Rain, P., Espilit, T., Francois, S. (2015). Determination of the aging mechanism of single core cables with PVC insulation. Polymer Degradation and Stability, 119: 96-104. https://doi.org/10.1016/j.polymdegradstab.2015.05.008
[39] Morel, J.F., Dung, P.N., Joly, J.C. (1980). Thermal aging of bi-axially orifnted pet films: Relation between structural changes and dielectric behavior. IEEE Transactions on Electrical Insulation, (4): 335-339. https://doi.org/10.1109/TEI.1980.298260